International Journal of the Korean Society of Precision Engineering, Vol. 2, No. 4, November 2001.

Motion Analysis of a Translating Flexible Beam Carrying a Moving Mass

Sangdeok Park[1] and Youngil Youm[2]

[1] Mechatronics Research Team, Research Institute of Industrial Science and Technology, Pohang, South Korea
[2] Robotics and Bio-Mechatronics Lab., Department of Mechanical Engineering, POSTECH, Pohang, South Korea

ABSTRACT

This paper investigates vibrational motion of a flexible beam fixed on a moving cart and carrying a moving mass. The equations of motion of the beam-mass-cart system are analyzed through the unconstrained modal analysis. The exact normal mode solutions used in modal analysis correspond to the eigenfrequencies for each position of the moving mass and to the ratios of the weight of the beam-mass-cart system. Time solutions of normal modes are also transformed properly according to the position of the moving mass. Numerical simulations are carried out to obtain open-loop responses of the system in tracking pre-designed paths of the moving mass. The simulation results show that the model predicts the dynamic behavior of the beam-mass-cart system well. Experiments are carried out to show the validity of the proposed analytical method.

Keywords : Flexible beam, Moving mass, Unconstrained modal analysis, Frequency equation

1. Introduction

In the past, there have been reported a lot of research works on dynamic analysis of an elastic beam with a moving force or mass. Initially, the problem of moving mass load on an elastic beam is originated mainly from the applications in the field of transportation such as bridges, railways and guide ways supporting a moving mass load.

As the historical review of the latter half of last century, Ayre et al. [1] studied the effect of the ratio of the weight of a load to the weight of a simply supported beam for a constantly moving mass load. Kenney [2] found the possible velocities for the propagation of free bending waves and studied their relation to the critical velocity of the beam. Steele [3] investigated the series solution of a finite, simply supported Euler-Bernoulli beam, with and without an elastic foundation. Nelson and Conover [4] analyzed the dynamic stability of the lateral response of a simply supported Bernoulli-Euler beam carrying a continuous series of equally spaced mass particles. Stanišić and Hardin [5] developed a theory describing the response of a beam to an arbitrary number of moving masses by using Fourier finite sine transforms. Ting et al. [6] developed an algorithm to solve the dynamic response of a finite elastic beam supporting a constantly moving mass.

Relevant to the research works after 1990s, Olsson [7] presented analytical and finite element solutions to the dynamic problem of a simply supported beam subjected to a constant force moving at a constant speed. Mackertich [8] presented the response of a beam to a constant moving mass utilizing the beam theory with corrections for the shear deformation and rotary inertia. Lee [9] formulated the equation of motion for an Euler beam acted upon by a concentrated mass moving at a constant speed by using the Lagrangian approach and the assumed mode method. Lee [10] investigated the onset of the separation between the moving mass and beam and took into account its effect on calculating the interact force and the dynamic responses of the beams. Foda and Abduljabbar [11] presented an exact and direct modeling technique based on the dynamic Green function for

modeling beam structures subjected to a mass moving at constant speed.

All the above works dealt with simply supported or cantilevered beams with constantly moving masses or forces because the main purpose of those works was the vibration analysis of bridges, railroads or guide ways on which the moving mass load or force passes. When an elastic beam carrying a moving mass, however, is fixed on a moving cart and if the total mass of the beam and the moving mass can not be negligible compared with that of the cart, then the motion of the beam-mass system affects that of the cart, and vice versa. Therefore, in this case, the total dynamics of the beam-mass-cart system should be considered.

For example, when the stacker cranes in automatic warehouses, high tower cranes, ladder cars or overhead cranes move a heavy load, the vibrational motions due to the flexibility of the main beam are unavoidable. Furthermore, when the load moves along the flexible beam, the vibrational motions vary with the position of the load and the ratios of the weight of the beam-mass-cart system [12]. Therefore, the rigid body motion of the cart as well as the vibrational motion of the beam-mass system should be included in the analysis to analyze the total motion of the beam-mass-cart system.

In this paper, the vibrational motion of a Bernoulli-Euler beam fixed on a moving cart and carrying a moving mass along the beam is analyzed. The differences, both in modeling and analysis, between the previous works and this one are: (1) The flexible beam considered herein is fixed on a moving cart. That is, it is not restrained at a large reference frame. Therefore, the total dynamics of the beam-mass-cart system is considered in deriving the equations of motion. (2) The velocities of the moving mass and the cart are not constants. (3) At every position of the moving mass, the exact normal mode solutions corresponding to the eigenfrequencies of the beam-mass-cart system are used. (4) Proper transformations of the time solutions between normal modes for a position and those for the next position of the moving mass are adopted.

In the following section the equations of motion of the beam-mass-cart system are derived, and the modal analysis is described in section 3. Numerical simulations for the open-loop responses of the system in tracking the pre-designed path of the moving mass are performed in section 4, some experimental results are presented in section 5, and followed by conclusions.

2. Mathematical Modeling

Stacker cranes in automated warehouses can be modeled as a Bernoulli-Euler beam fixed on a moving cart and carrying a moving mass as shown in Fig. 1. The cart moves on the horizontal plane by the applied force $f_1(t)$. The mass moves along the beam by the friction wheels driven by a motor.

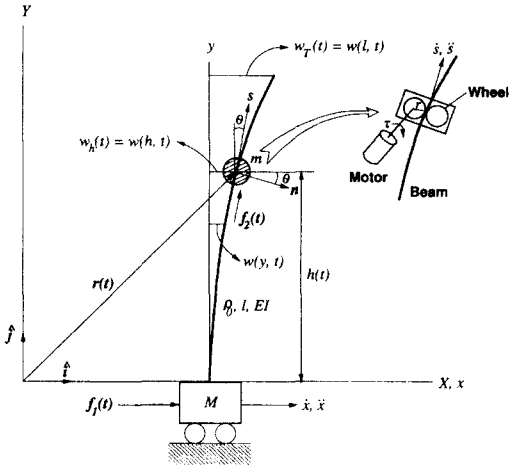

Fig. 1 The beam-mass-cart system considered.

To derive the equations of motion of the beam-mass-cart system, the following assumptions are made: (1) The driving force for the cart, $f_1(t)$, is applied to $\hat{i}$ - direction. (2) The local driving force for the moving mass is generated by the driving motor of the moving mass as $f_2(t) = \tau(t)r$, where $\tau(t)$ is the torque by the driving motor for the moving mass and r is the radius of the driving wheel of the moving mass. (3) The moving mass is not separated from the beam. (4) There is no longitudinal deflection of the beam, thus only the lateral deflection is possible. (5) The lateral deflection of the beam is small compared with the length of the beam. (6) The rotational effect of the moving mass and the beam with respect to the local coordinate system is neglected. (7) All the motion occurs in XY plane, and the system is not fallen down.

Under these assumptions, the equations of motion and the boundary conditions are obtained as follows:

$$M\ddot{x} + \int_0^l \{[\rho_0 + m\delta(y-h)](\ddot{x}+\ddot{w}) + m\delta(y-h)[\ddot{h}w' + 2\dot{h}\dot{w}' + \dot{h}^2 w'']\} dy = f_1(t), \quad (1)$$

$$EIw'''' + [\rho_0 + m\delta(y-h)](\ddot{x}+\ddot{w}) + m\delta(y-h)[\ddot{h}w' + 2\dot{h}\dot{w}' + \dot{h}^2 w''] = 0, \quad (2)$$

$$m\{\ddot{h} + (\ddot{x} + \ddot{w}_h + \dot{h}^2 w_h'' + 2\dot{h}\dot{w}_h')w_h' + g\} = f_2(t), \quad (3)$$

and

$$w(0,t) = w'(0,t) = EIw''(l,t) = EIw'''(l,t) = 0, \quad (4)$$

where $w(y, t)$ is the deflection of the beam at y, $w_h(t) = w(h(t), t)$ is the deflection of the flexible beam at $y = h(t)$, M is the mass of the cart, EI is the flexural rigidity of the beam, ρ_0 is the mass per unit length of the flexible beam without the moving mass, m is the mass of the moving mass, $\dot{w} = \partial w(y,t)/\partial t$ and $w'' = \partial^2 w(y,t)/\partial t^2$.

Eq. (1) contains x-directional inertial force of the beam-mass-cart system, the inertial forces of the beam and the mass due to the deflection of the beam and those by linear, Coriolis and centripetal accelerations of the moving mass. Eq. (2) is exactly the same as the results in references [6, 9, 10, 16] except the x-directional acceleration term of the loaded beam. Eq. (3) describes the motion of the moving mass by the applied force, $f_2(t)$, and by the motion of the elastic beam. In this study the coupled equations (1)-(3) are solved simultaneously utilizing the *unconstrained modal analysis* [19, 20] in the next section assuming that the vertical position of the moving mass is given previously.

3. Modal Analysis

To solve the partial differential equations given (2), some investigators used influence functions, Green functions [6, 10, 11], sine series [5, 7, 15] or assumed mode functions [9]. In separating the deflection of an elastic beam into time solutions and mode solutions, many authors used the normal modes of the beam without the moving mass (*for example, see references* [9, 10]). However, the normal mode functions used in above works do not represent the exact mode solutions because the natural frequencies and the corresponding normal mode solutions of the beam are changed as the position of the concentrated mass changes [12].

When one tries to solve the coupled equations of motion utilizing modal analysis, it is impossible to separate the variables of the elastic deflection of the beam by the proper mode functions and time functions because the vibration characteristics of a beam with a moving mass change along the position of the mass while the method of separation of variables is focused on the constant link length. Examples of this kind of system can be seen in references [17] and [18].

In this approach, to solve the coupled equations of motion using unconstrained modal analysis, exact normal mode solutions corresponding to the frequency characteristics for the position of the moving mass and the weight ratios of the beam-mass-cart system are used under the following assumptions.

Assumptions: *1) If the magnitudes of the vertical velocity and acceleration of the moving mass are small as* $\dot{h}/l << \omega_{fund}$ *and* $\ddot{h}/l << \omega_{fund}^2$, *where* ω_{fund} *is the fundamental frequency of the beam-mass-cart system, then, at a certain time t, the moving mass is considered to be fixed at* $\bar{h}$ *during a small time interval* Δt *while* $\dot{h}$ *and* $\ddot{h}$ *are still valid. 2) The beam oscillates in the same manner during this time interval.*

In the above assumptions, $\dot{h}/l << \omega_{fund}$ and $\ddot{h}/l << \omega_{fund}^2$ are reasonable in many industrial applications because the speed of the moving mass is relatively small compared with the vibration frequency of the beam. Under these assumptions, we can find the natural frequencies and corresponding normal mode solutions for the system which has a fixed mass at an arbitrary position $\bar{h}^o$. Then, we solve the original equations of motion several times utilizing these mode solutions during $\bar{h}^o \le h(t) < \bar{h}^o + \Delta h$ while updating $\dot{h}(t)$ and $\ddot{h}(t)$ at every Δt. If $h(t) \ge \bar{h}^o + \Delta h = \bar{h}^n$, we find new natural frequencies and the corresponding normal modes with new position of the moving mass, $\bar{h}^n$. Then, we solve the original equations of motion again utilizing these updated mode solutions and proper transformation of time solution during $\bar{h}^n \le h(t) < \bar{h}^n + \Delta h$.

The equations of motion for the beam-mass-cart system with a fixed mass at $\bar{h}$ are given as follows[12]:

$$M\ddot{x} + \int_0^l [\rho_0 + m\delta(y-\bar{h})](\ddot{x}+\ddot{w})\, dy = f_1(t), \quad (5)$$

$$EIw'''' + [\rho_0 + m\delta(y-\bar{h})](\ddot{x}+\ddot{w}) = 0, \quad (6)$$

and the boundary conditions (4).

By *unconstrained modal analysis*, the deflection of he beam at y, $w(y, t)$, and the position of the cart, $x(t)$, can be represented, respectively, as [19, 20]:

$$w(y,t) = \sum_{i=1}^{\infty} \phi(y) q(t) \tag{7}$$

and

$$x(t) = \alpha(t) + \sum_{i=1}^{\infty} \beta q(t), \tag{8}$$

where $\alpha(t)$ describes the motion of the center of mass of the total system without perturbation, and

$$\phi_i(y) = \psi_i(y) - \beta_i, \tag{9}$$

where

$$\psi_i(y) = \left[A_i(y) + \frac{C_i}{1 - D_i} B_i(y) \right] \psi_i(\bar{h}), \tag{10}$$

and

$$\beta_i = -\frac{m}{M} \psi_i(\bar{h}) - \frac{\rho_0}{M} \int_0^l \psi_i(y) dy, \tag{11}$$

where $A_i(y)$, $B_i(y)$, C_i, D_i and $\psi_i(\bar{h})$ for each eigenvalue k_i are given in Appendix. The eigenvalues k_i are the roots of the frequency equation [12]:

$$\begin{aligned} & 1 + \cos\xi \cosh\xi \\ & + \frac{r_1}{4} \left[\cos\xi \cosh(\xi - 2\eta) + \cos(\xi - 2\eta) \cosh\xi \right. \\ & \quad + \sin\xi \sinh(\xi - 2\eta) - \sin(\xi - 2\eta) \sinh\xi \\ & \quad \left. + 2\cos\xi \cosh\xi + 4\cos\eta \cosh\eta \right] \\ & + \frac{r_2}{\xi} \left(\sin\xi \cosh\xi + \cos\xi \sinh\xi \right) \\ & + \frac{r_3 \xi}{4} \left[2\sin(\xi - \eta) \cosh(\xi - \eta) - 2\sin\eta \cosh\eta \right. \\ & \quad - 2\cos(\xi - \eta) \sinh(\xi - \eta) + 2\cos\eta \sinh\eta \\ & \quad + \cos(\xi - 2\eta) \sinh\xi + \cos\xi \sinh\xi \\ & \quad \left. - \sin\xi \cosh(\xi - 2\eta) - \sin\xi \cosh\xi \right] = 0, \end{aligned} \tag{12}$$

where $r_1 = m/M$, $r_2 = m_b/M$, $r_3 = m/m_b$, $m_b = \rho_0 l$, $\xi = kl$ and $\eta = k\bar{h}$. Using the normal mode solution (9) we solve (1)-(3) during $\bar{h} \le h(h) < \bar{h} + \Delta h$.

If (11) is satisfied, the motion of the center of mass for $h(t) = \bar{h}$ is obtained as:

$$\begin{aligned} M_t \ddot{\alpha}(t) + m \Big[& \ddot{h}(t) \sum_{i=1}^{\infty} \phi_i'(\bar{h}) q_i(t) + 2\dot{h}(t) \sum_{i=1}^{\infty} \phi_i'(\bar{h}) \dot{q}_i(t) \\ & + \dot{h}^2(t) \sum_{i=1}^{\infty} \phi_i''(\bar{h}) q_i(t) \Big] = f_1(t), \end{aligned} \tag{13}$$

where $M_t = M + m + m_b$ is the total mass of the beam-mass-cart system.

Meanwhile, $\psi_i(y)$ in (9) and (10) satisfies [12]:

$$EI \psi_i''''(y) - \omega_i^2 \bar{\rho} \psi_i(y) = 0, \tag{14}$$

and

$$\int_0^l \bar{\rho} \phi_i(y) \psi_j(y) = \delta_{ij}, \tag{15}$$

where

$$\omega_i^2 = \frac{EIk_i^4}{\rho_0}, \tag{16}$$

$\bar{\rho} = \rho_0 + m\delta(y - \bar{h})$ and δ_{ij} is the *Kronecker delta*. From (2), (7), (8) and (13)-(15), one obtains

$$\begin{aligned} & \ddot{q}_i(t) + \omega_i^2 q_i(t) + m \psi_i(\bar{h}) \Big[\ddot{h}(t) \sum_{j=1}^{\infty} \phi_j'(\bar{h}) q_j(t) \\ & + 2\dot{h}(t) \sum_{j=1}^{\infty} \phi_j'(\bar{h}) \dot{q}_j(t) + \dot{h}^2(t) \sum_{j=1}^{\infty} \phi_j''(\bar{h}) q_j(t) \Big] \\ & = \beta_j f_1(t). \end{aligned} \tag{17}$$

The time solution for the moving mass located at $\bar{h} \le h(h) < \bar{h} + \Delta h$ can be found as (17). If the position of the mass is changed sufficiently large enough that it must be updated, then the natural frequencies and the corresponding normal modes for the position $\bar{h}$ are no longer valid. In this case, we should find new natural frequencies and the corresponding normal modes with updated position of the moving mass. Then we solve the original equations of motion and the time solutions, (17). again using the updated mode solutions.

In calculating the time solutions with new mode solutions, however, there must be proper transformations between old time solutions and new ones. If the position of the moving mass is changed from $\bar{h}^o$ to $\bar{h}^n = \bar{h}^o + \Delta h$ at any time instant t, then the deflection of the beam at this time can be represented by using either $\bar{h}^o$ or $\bar{h}^n$ as

follows:

$$w(y,t)=\sum_{i=1}^{\infty}q_i^o(t)\phi_i^o(y)=\sum_{j=1}^{\infty}q_j^n(t)\phi_j^n(y), \tag{18}$$

where $\phi_i^o(y)$ and $\phi_j^n(y)$ are the normal mode solutions corresponding to the eigenfrequencies for the position $\bar{h}^o$ and $\bar{h}^n$, respectively. The error between the two expressions (18) will be checked in the next section.

Multiplying both sides of Eq. (18) by $\bar{\rho}^n\psi_j^n(y)$, integrating over the problem domain and applying the orthogonality condition (15), one can obtain the transformation between old time solutions and new ones as follows:

$$q_j^n(t)=\sum_{i=1}^{\infty}q_i^o(t)\int_0^l\bar{\rho}^n(y)\phi_i^o(y)\psi_j^n(y)dy, \tag{19}$$

where $\bar{\rho}^n=\rho_0+m\delta(y-\bar{h}^n)$. Eq. (19) is used to transform the time solutions when the natural frequencies and the corresponding mode solutions for $\bar{h}^o$ are changed to those for $\bar{h}^n$.

For numerical simulations, a *finite-dimensional* approximated model for a finite number of mode solutions is considered from the previous development by taking the first p expansions in (7) and (8) as follows:

$$w(y,t)=\sum_{i=1}^{p}\phi_i(y)q_i(t), \tag{20}$$

and

$$x(t)=\alpha(t)+\sum_{i=1}^{p}\beta_i q_i(t). \tag{21}$$

4. Numerical Examples

4.1 Linear motion of a moving mass

Numerical simulations are carried out to obtain open-loop responses of the beam-mass-cart system when the moving mass follows pre-designed paths by several ways. At first, the forcing function $f_1(t)$ given by

$$f_1(t)=\begin{cases}20N & \text{when } 0<t\le 0.2\\ -20N & \text{when } 1.0<t\le 1.2\\ 0 & \text{otherwise}\end{cases} \tag{22}$$

is applied to the cart while $f_2(t)$ is pre-designed to generate the trajectory of the moving mass as given in Fig. 2.

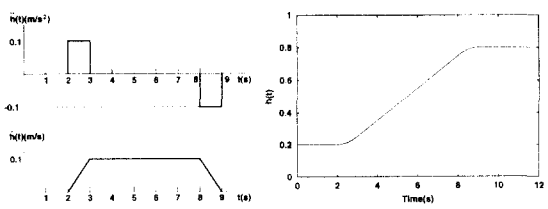

(a) Acceleration and velocity profiles (b) Position profile

Fig. 2 Acceleration, velocity and position profiles of the moving mass for upward motion.

Table 1 System parameters for numerical simulations.

Parameters	Value
Mass of cart, M	$10.0kg$
Length of elastic beam, l	$1.0m$
Mass per unit length of beam, ρ_0	$0.788kg/m$
Young's modulus of beam, E	$2.07\times10^{11}N/m^2$
Area moment of inertia, I	$5.208\times10^{-11}m^4$

Fig. 3 shows the position of the cart, $x(t)$, the global position of the moving mass, $x_h(t)$, the global position of the tip of the elastic beam, $x_T(t)$, the local deflection of the beam at which the moving mass is located, $w_h(t)$, and the local deflection of the beam at the tip of the beam, $w_T(t)$, respectively, where $x_h(t) = x(t) + w_h(t)$ and $x_T(t) = x(t) + w_T(t)$, when $m = 2kg$, $\Delta h = l/200$, $p = 3$ and the system parameters given in Table 1 are used.

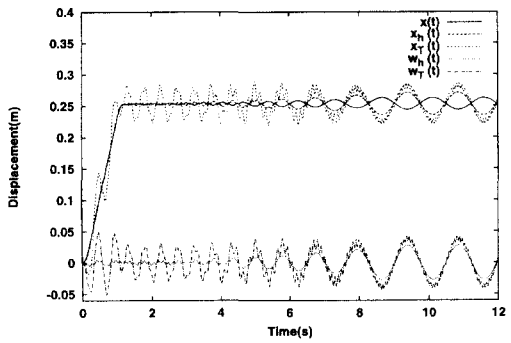

Fig. 3 Open-loop response of the beam-mass-cart system to the forcing function (22) and the trajectory of moving mass in Fig. 2 when $m = 2kg$.

As seen in Fig. 3, the deflection at $y = h$, $w_h(t)$, becomes large as the moving mass moves from $h = 0.2$ to

0.8 while the tip deflection, $w_T(t)$, at steady state is bounded within $\pm 0.031(m)$. It can be also known that the motion of the oscillating beam and the moving mass affects that of the cart, and vice versa. Furthermore, the fundamental frequency of the beam gets low as the position of the moving mass becomes high. The change of the fundamental frequency during this motion by Eq. (16) is from 2.106Hz(13.23 rad/s) to 0.914Hz(5.74 rad/s), and the conditions that $\dot{h}/l << \omega_{fund}$ and $\ddot{h}/l << \omega^2_{fund}$ in the Assumptions are sufficiently satisfied since $\dot{h}_{max} = 0.1m/s$, $\ddot{h}_{max} = 0.1m/s^2$, and l = $1m$ in this simulation.

In the numerical simulations, Δt is given as $\Delta t = 2\pi/100\omega_{fund}$, and, thus Δt varies from 4.74 $\times 10^{-3}s$ to 10.95 $\times$ $10^{-3}s$ while the moving mass moves from h = 0.2m to h = 0.8m. If the moving mass moves with the maximum velocity, the moving mass can move minimum 0.474mm to maximum 1.095mm during Δt . Therefore, the assumption that the moving mass is fixed at a certain position during Δt is valid. In this numerical simulation, the natural frequencies are updated at every Δh = l/200 = 5mm. In that case, for example, the fundamental frequency at h = 0.8m and h = 0.795m are 0.914Hz and 0.922Hz, respectively. Thus, the difference of fundamental frequencies between h = 0.8m and h = 0.795m is negligible. Furthermore, when the moving mass moves from h = 0.795m to h = 0.8m with the maximum velocity, it takes 0.05s = 5.422 Δt . Therefore, assumption that the beam oscillates in the same manner during Δt is valid.

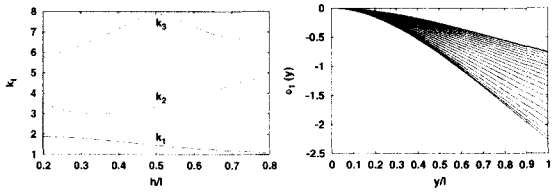

(a) Eigenfrequencies (b) The first mode shapes

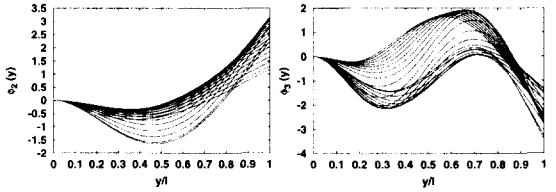

(c) The second mode shapes (d) The third mode shapes

Fig. 4 The first three roots of the frequency equation (12) and the selected corresponding mode shapes with respect to the change of the position of the moving mass when m = 2kg.

Fig. 4 shows the change of the first three roots of the frequency equation (12) and the selected corresponding mode shapes with respect to the change of the position of the moving mass, and that is the reason why the normal mode solutions should be updated at every position of the moving mass.

4.2 Circular motion of moving mass

The other numerical simulations are carried out to obtain the open-loop responses of the system in tracking the pre-designed circular path of the moving mass. The task is to draw a circle

$$(X - x_c)^2 + (Y - y_c)^2 = R^2 \tag{23}$$

in XY plane with the moving mass. Since the purpose of this study is to investigate the vibrational motion of an elastic beam, the desired path is planned without considering the flexibility of the elastic beam. The force to be applied to the cart, $f_1(t)$, is generated as

$$f_1(t) = M_t[\ddot{\alpha}_d + K_v(\dot{\alpha}_d - \dot{\alpha}) + K_p(\alpha_d - \alpha)] \tag{24}$$

to follow the desired trajectory of the center of mass of the moving mass as

$$\alpha_d(t) = x_c - R\sin(\Omega t), \tag{25}$$

because $\alpha(t) = x(t)$ in the case of rigid beam. Further, it is assumed that the force to be applied to the moving mass, $f_2(t)$, causes the desired vertical trajectory of the moving mass to follow

$$h_d(t) = y_c \pm R\cos(\Omega t). \tag{26}$$

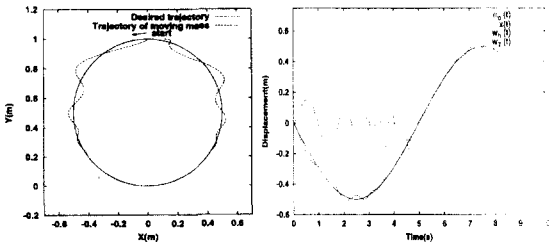

(a) Trajectory (b) Time response

Fig. 5 Trajectory of the moving mass and time response of the beam-mass-cart system when m = 5kg and $\Omega = 2\pi/10$.

Fig. 5 shows the simulated trajectory of the moving mass and the tip of the elastic beam with respect to the desired one in (a) and $x(t)$, w_h and $w_T(t)$ in (b) when m = 5kg, (x_c, y_c) = (0, 0.5)m, R = 0.5m, K_p = 15, K_v = 15, Δh = $l/200$, p = 3, $\Omega = 2\pi/10$ and the system parameters given in Table 1 are used. The moving mass moves to counter-clockwise direction from the start point (X, Y) = (0, 1). As seen in the results, w_h becomes smaller as the moving mass goes down from upper position to lower one while the vibration becomes fast.

5. Experimental Verification

5.1 Experimental setup

Fig. 6 shows the experimental setup. As seen in Figs. 6 (a) and (b), a thin flexible beam carrying a concentrated or a moving mass is clamped on the moving carriage of a linear motor by a beam fixture. The linear motor used as the moving base is LEB-S-2-S made by ANORAD Co. Fig. 6 (c) shows the moving mass. The moving mass moves along the flexible beam by two pairs of rubber-coated wheels driven by an AC servo motor and a reduction gear. Table 2 shows the specifications of the experimental setup.

Table 2 Specification of the experimental setup.

Moving base	Max. moving velocity	2.0m/s
	Max. moving distance	0.5m
	Resolution of encoder	2μm
	Mass of moving carriage	5.04kg
	Mass of beam fixture	4.61kg
Beam 1	Dimension($L\times W\times T$)	1000×50×3.12mm
	Mass per unit length	1.1268kg/m
	Area moment of inertia	$1.265\times10^{-10}m^4$
	Young's modulus	$2.07\times10^{11}N$
Beam 2	Dimension($L\times W\times T$)	1000×49.85×3.8
	Mass per unit length	1.4776kg/m
	Area moment of inertia	$2.279\times10^{-10}m^4$
	Young's modulus	$2.07\times10^{11}N$
Moving mass	Servo motor power	100W
	Servo motor torque	0.32N/m
	Servo motor speed	3000rev/min
	Gear reduction rate	10 : 1
	Total weight	5.4kg

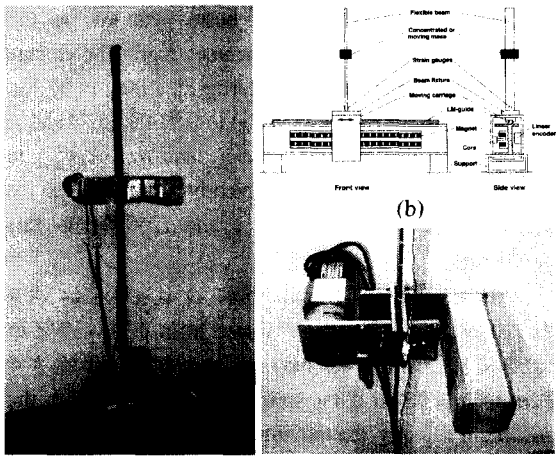

Fig. 6 Experimental setup: (a) Photograph, (b) Schematic diagram, (c) The moving mass.

5.2 Linear motion of the moving mass

The open-loop responses of the beam-mass-cart system with a linearly moving mass are verified by experiments. For these experiments, the base cart on which the beam 1 in Table 2 carrying the moving mass is mounted is excited by the driving force

$$f_1(t) = \begin{cases} 30N & \text{when } 0 < t \le 0.2\text{s} \\ 0N & \text{when } t > 0.2\text{s}. \end{cases} \quad (27)$$

The moving mass was controlled by the RIC (Robust Internal-loop Compensator) [22] to robustly follow given trajectories even under the disturbances such as friction and the dynamics due to the vibration of the beam.

Fig. 7 shows the open-loop response of the beam-mass-cart system when the moving mass follows the trajectory Fig. 7 (c) along the flexible beam. Fig. 7 (a) is the global trajectory of the moving mass in XY plane after the moving base stops. The trajectory was obtained by taking a picture of an LED attached to the moving mass after the moving base is translated by the applied force. The upper semi-arc line is caused by the other LED attached to the top end of the beam. Fig. 7 (b) is the position of the cart measured by the linear encoder of the

linear motor. As seen in Fig. 7 (b), the cart stops at a position without the deceleration command due to the friction between the moving carriage and the LM-guide of the linear motor. Fig. 7 (c) is the time trajectory of the moving mass measured by the encoder of the servo motor of the moving mass. The maximum error between the reference trajectory and the measured one in this experiment is less than $0.7mm$ in spite of the large friction between the flexible beam and the moving mass. Fig. 7 (d) is the strain signal measured by strain gauges attached to the root of the flexible beam.

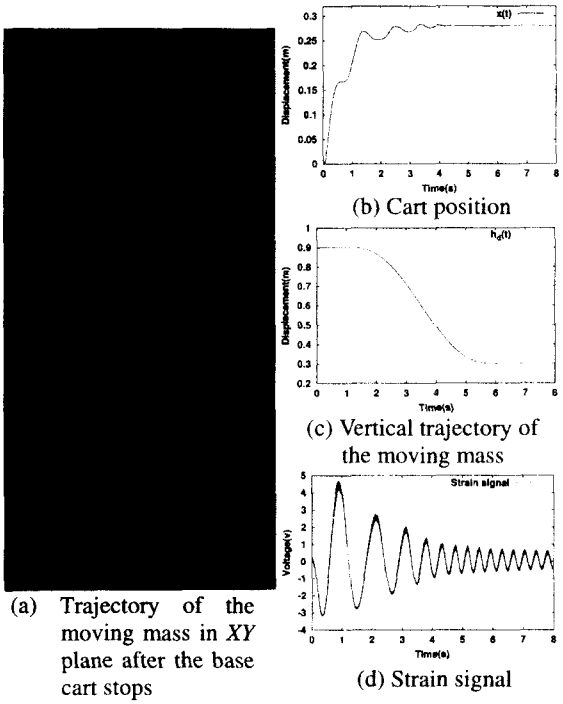

(a) Trajectory of the moving mass in XY plane after the base cart stops

(b) Cart position

(c) Vertical trajectory of the moving mass

(d) Strain signal

Fig. 7 Open-loop responses for the linear motion of the moving mass.

Fig. 8 shows the simulation results for the same conditions as the previous experiment. In this simulation the friction force between the moving carriage and the LM-guide of the linear motor is modeled as

$$F_{fric} = \begin{cases} 0 & \text{when} \quad \dot{x} = 0 \\ f_{st} \cdot \mathrm{sgn}(\dot{x}) & \text{when} \quad 0 \le |\dot{x}| \le \varepsilon \\ f_c \cdot \mathrm{sgn}(\dot{x}) + f_v \dot{x} & \text{when} \quad |\dot{x}| > \varepsilon, \end{cases} \tag{28}$$

where f_{st} and f_c are the static and the Coulomb friction forces, respectively, f_v is the viscous friction coefficient, and ε is a positive infinitesimal value. The friction coefficients used in these simulations are f_{st} = 5.0, f_c = 3.5, and f_v = 2.35. Considering that the friction coefficients have some error and that the natural frequencies of the system differ a little from those by (16) and (12) due to the friction force [12], the simulation results match precisely with those of experiments, especially for the cart positions and the tip deflections.

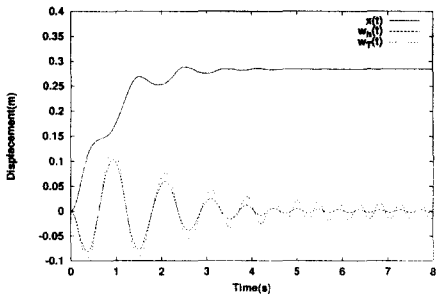

Fig. 8 Simulation results for the linear motion of the moving mass.

5.3 Circular motion of the moving mass

The responses of the beam-mass-cart system for the circular motion of the moving mass in XY plane are verified by experiments. For these experiments, the base cart on which the beam 2 is mounted is controlled by the controller

$$f_1(t) = M_t[\ddot{x}_d + K_v(\dot{x}_d - \dot{x}) + K_p(x_d - x)]. \tag{29}$$

The desired trajectory of the base cart is designed as

$$x_d(t) = x_c - R\sin\Omega t, \tag{30}$$

and it is assumed that the RIC makes the moving mass to follow the trajectory

$$h_d(t) = y_c + R\cos\Omega t. \tag{31}$$

Fig. 9 (a) shows the experimental results when the moving mass follows the circular path given by (30) and (31) with radius R = 0.2 and $\Omega = 2\pi/5$. The moving mass starts from (x_c, y_c) = (0.0, 0.9) to CCW direction, and the feedback gains K_p and K_v are 250 and 7.5, respectively. Fig. 9 (b) is the simulation results using the proposed analytical method for the same conditions as the previous experiment. Fig. 9 (c) and (d) are the same experiment and simulation results when K_p = 140.6 and

$K_v = 5.6$.

It is difficult to quantitatively compare the experimental results with those by simulation because of inaccuracy in measuring the global position of the moving mass. However, it can be known that the simulation results by the proposed analytical method describes the experimental results excellently except some difference in natural frequencies of the system.

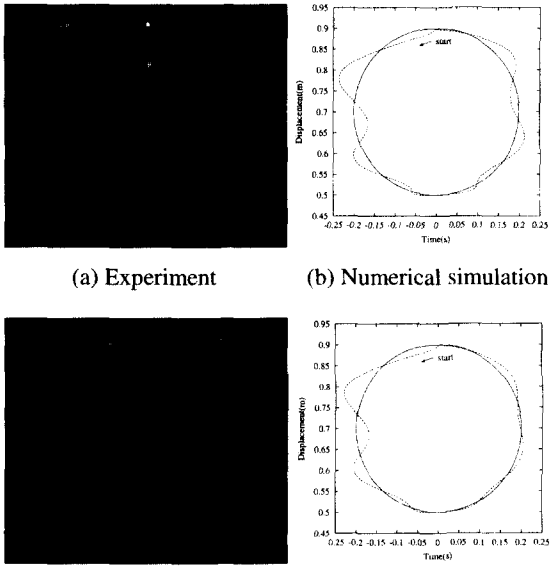

(a) Experiment (b) Numerical simulation

(c) Experiment (d) Numerical simulation

Fig. 9 Circular motion of the moving mass when $R = 0.2$, $\Omega = 2\pi/5$. (a) and (b) $K_p = 250$ and $K_v = 7.5$, (c) and (d) $K_p = 140.6$ and $K_v = 5.6$.

6. Concluding Remarks

In this study, we derived the equation of motion of an elastic beam fixed on a moving cart and carrying a moving mass, and solved the coupled dynamic equations using the unconstrained modal analysis. We also proposed an analytical method utilizing the exact normal mode solutions corresponding to the eigenfrequencies for the position of the moving mass and the ratios of the weight of the beam-mass-cart system. In the analysis we adopted the proper transformation of the time solutions between the normal modes for a position and those for the next position of the moving mass.

Numerical simulations were carried out to verify the validity of the proposed method, and the open-loop responses of the system in tracking the pre-designed path of the moving mass were obtained. The simulation results accurately predicts the dynamic behavior of the beam-mass-cart system well and this method can be used as a motion simulator which describes the vibrational motion of a moving elastic beam with a moving mass. Those analytical results were compared with experimental ones. The experimental results show the validity of the analytical method proposed in this study.

References

1. Ayre, R. S., Jacobsen, L. S., and Hsu, C. S., "Transverse Vibration of One- and of Two-Span Beams Under the Action of a Moving Mass Load," Proceedings of the First U.S. National Congress of Applied Mechanics, pp.81-90, 1951.
2. Kenney, J. T. Jr., "Steady-State Vibrations of Beam on Elastic Foundation for Moving Load," ASME Journal of Applied Mechanics, Vol. 21, pp.359-364, 1954.
3. Steele, C. R., "The Finite Beam With a Moving Mass," ASME Journal of Applied Mechanics, Vol. 34, pp.111-118, 1967.
4. Nelson, H. D., and Conover, R. A., "Dynamic Stability of a Beam Carrying Moving Masses," ASME Journal of Applied Mechanics, Vol. 93, pp.1003-1006, 1971.
5. Stanišić, M. M., and Hardin, J. C., "On the Response of Beams to an Arbitrary Number of Concentrated Moving Mass," Journal of The Franklin Institute, Vol. 287, pp.115-123, 1969.
6. Ting, E. C., Genin, J., and Ginsberg, J.H., "A General Algorithm for Moving Mass Problems," Journal of Sound and Vibration, Vol. 33, pp.49-58, 1974.
7. Olsson, M., "On the Fundamental Moving Load Problem," Journal of Sound and Vibration, Vol. 145, pp.299-307, 1991.
8. Mackertich, S., "Response of a Beam to a Moving Mass," Journal of Acoustical Society of America, Vol. 92, pp.1766-1769, 1992.
9. Lee, H. P., "Dynamic Responses of a Beam With a Moving Mass," Journal of Sound and Vibration, Vol. 191, pp.289-294, 1996.
10. Lee, U., "Separation Between the Flexible Structure

and the Moving Mass Sliding on It," Journal of Sound and Vibration, Vol. 209, pp.867-877, 1998.

11. Foda, M. A., and Abduljabbar, Z., "A Dynamic Green Function Formulation for the Response of a Beam Structure to a Moving Mass," Journal of Sound and Vibration, Vol. 210, pp.295-306, 1998.
12. Park, S., Chung, W. K., Youm, Y., and Lee, J. W., "Natural Frequencies and Open-Loop Responses of an Elastic Beam Fixed on a Moving Cart and Carrying an Intermediate Lumped Mass," Journal of Sound and Vibration, Vol. 230, pp.591-615, 2000.
13. Meirovitch, L., *Computational Methods in Structural Dynamics*, Maryland: SIJTHOFF & NOORDHOFF, 1980.
14. Meirovitch, L., "Derivation of Equations for Flexible Multibody Systems in Terms of Quasi-Coordinates from the Extended Hamilton's Principle," Shock and Vibration, Vol. 1, pp.107-119, 1993.
15. Stanišić, M. M., and Montgomery, S. T., "On a Theory Concerning the Dynamical Behavior of Structures Carrying Moving Masses," Ingenieur-Archiv, Vol. 43, pp.295-305, 1974.
16. Lee, U., Park, C. H., and Hong, S. C., "The Dynamics of a Piping System With Internal Unsteady Flow," Journal of Sound and Vibration, Vol. 180, pp.297-311, 1995.
17. Fung, R.-F., Lu, P.-Y., and Tseng, C.-C., "Non-Linearly Dynamic Modeling of an Axially Moving Beam With a Tip Mass," Journal of Sound and Vibration, Vol. 218, pp.559-571.
18. Yamazaki, H., Ono, T., and Park, C. Y., "Trajectory Control of the Flexible Manipulator With Time-Varying Arm," Proceedings of the 11th Korea Automatic Control Conference(KACC), pp.405-408, 1996.
19. Barbieri, E., and Özgüner, Ü., "Unconstrained and Constrained Mode Expansion for a Flexible Slewing Link," Transaction of Dynamic System Measurement and Control, Vo l. 110, pp.416-421, 1988.
20. de Wit, C. C., Siciliano, B., and Bastin, G., *Theory of Robot Control*, Springer-Verlag Berlin Heidelberg New York, 1996.
21. Sadiku, S., and Leipholz, H.H.E., "On the Dynamics of Elastic Systems With Moving Concentrated Masses," Ingenieur-Archiv, Vol. 57, pp.223-242, 1987.
22. Kim, B. K., Choi, H. T., Chung, W. K., and Chang, Y. H., "Robust Optimal Internal Loop Compensator Design for Motion Control of Precision Linear Motor," Proceedings of IEEE International Symposium on Industrial Electronics, pp.1045-1050, 1999.

Appendix

In Eq. (10),

$$A_i(y)=\frac{m\omega_i^2}{4EIk_i^3}\left\{\frac{\mathrm{c}k_i y-\mathrm{ch}k_i y}{1+\mathrm{c}k_i l\,\mathrm{ch}k_i l}\right.$$
$$\times\left[\left(\mathrm{s}k_i(l-\bar{h})+\mathrm{sh}k_i(l-\bar{h})\right)(\mathrm{c}k_i l+\mathrm{ch}k_i l)\right.$$
$$\left.-\left(\mathrm{c}k_i(l-\bar{h})+\mathrm{ch}k_i(l-\bar{h})\right)(\mathrm{s}k_i l+\mathrm{sh}k_i l)\right]$$
$$+\frac{\mathrm{s}k_i y-\mathrm{sh}k_i y}{1+\mathrm{c}k_i l\,\mathrm{ch}k_i l} \qquad (A.1)$$
$$\times\left[\left(\mathrm{s}k_i(l-\bar{h})+\mathrm{sh}k_i(l-\bar{h})\right)(\mathrm{s}k_i l-\mathrm{sh}k_i l)\right.$$
$$\left.+\left(\mathrm{c}k_i(l-\bar{h})+\mathrm{ch}k_i(l-\bar{h})\right)(\mathrm{c}k_i l+\mathrm{ch}k_i l)\right]$$
$$\left.-2U(y-\bar{h})\left[\mathrm{s}k_i(y-\bar{h})-\mathrm{sh}k_i(y-\bar{h})\right]\right\},$$

$$B_i(y)=\frac{1}{2}\left[\mathrm{c}k_i y+\mathrm{ch}k_i y\right.$$
$$-\frac{\mathrm{s}k_i l\,\mathrm{sh}k_i l}{1+\mathrm{c}k_i l\,\mathrm{ch}k_i l}(\mathrm{c}k_i y-\mathrm{ch}k_i y) \qquad (A.2)$$
$$\left.+\frac{\mathrm{c}k_i l\,\mathrm{sh}k_i l+\mathrm{s}k_i l\,\mathrm{ch}k_i l}{1+\mathrm{c}k_i l\,\mathrm{ch}k_i l}(\mathrm{s}k_i y-\mathrm{sh}k_i y)\right],$$

$$C_i=-\frac{m}{2M}\frac{1}{1+\mathrm{c}k_i l\,\mathrm{ch}k_i l}$$
$$\times\left\{\left[\mathrm{c}k_i(l-\bar{h})+\mathrm{ch}k_i(l-\bar{h})\right](\mathrm{c}k_i l+\mathrm{ch}k_i l)\right. \qquad (A.3)$$
$$\left.+\left[\mathrm{s}k_i(l-\bar{h})+\mathrm{sh}k_i(l-\bar{h})\right](\mathrm{s}k_i l-\mathrm{sh}k_i l)\right\},$$

$$D_i=-\frac{\rho_0}{Mk_i}\frac{\mathrm{s}k_i l\,\mathrm{ch}k_i l+\mathrm{c}k_i l\,\mathrm{sh}k_i l}{1+\mathrm{c}k_i l\,\mathrm{ch}k_i l}, \qquad (A.4)$$

and

$$\psi_i(h)=\left\{m\left(1-\frac{C_i}{1-D_i}\right)\right.$$
$$\left.+\rho_0\int_0^l F_i(y)\left[F_i(y)-\frac{C_i}{1-D_i}\right]dy\right\}^{-\frac{1}{2}}, \qquad (A.5)$$

where $\mathrm{c}\equiv\cos$, $\mathrm{s}\equiv\sin$, $\mathrm{ch}\equiv\cosh$, $\mathrm{sh}\equiv\sinh$ and

$$F_i(y)=A_i(y)+\frac{C_i}{1-D_i}B_i(y) \qquad (A.6)$$